International Endodontic Journal

doi:10.1111/iej.12013

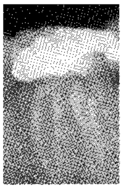

CASE REPORT

The diagnosis and conservative treatment of a complex type 3 dens invaginatus using cone beam computed tomography (CBCT) and 3D plastic models

A. Kfir[1], Y. Telishevsky-Strauss[1], A. Leitner[2] & Z. Metzger[1]

[1]Department of Endodontology, Tel Aviv University, Tel Aviv; and [2]Panorama, Naharya, Israel

Abstract

Kfir A, Telishevsky-Strauss Y, Leitner A, Metzger Z. The diagnosis and conservative treatment of a complex type 3 dens invaginatus using cone beam computed tomography (CBCT) and 3D plastic models. *International Endodontic Journal*, **46**, 275–288, 2013.

Aim To investigate the use of 3D plastic models, printed from cone beam computed tomography (CBCT) data, for accurate diagnosis and conservative treatment of a complex case of dens invaginatus.

Summary A chronic apical abscess with a draining sinus tract was diagnosed during the treatment planning stage of orthodontic therapy. Radiographic examination revealed a large radiolucent area associated with an invaginated right maxillary central incisor, which was found to contain a vital pulp. The affected tooth was strategic in the dental arch. Conventional periapical radiographs provided only partial information about the invagination and its relationship with the main root canal and with the periapical tissues. A limited-volume CBCT scan of the maxilla did not show evidence of communication between the infected invagination and the pulp in the main root canal, which could explain the pulp vitality. A novel method was adopted to allow for instrumentation, disinfection and filling of the invagination, without compromising the vitality of the pulp in the complex root canal system. The CBCT data were used to produce precise 3D plastic models of the tooth. These models facilitated the treatment planning process and the trial of treatment approaches. This approach allowed the vitality of the pulp to be maintained in the complex root canal space of the main root canal whilst enabling the healing of the periapical tissues.

Key learning points

- Even when extensive periapical pathosis is associated with a tooth with type III dens invaginatus, pulp sensibility tests should be performed.
- CBCT is a diagnostic tool that may allow for the management of such teeth with complex anatomy.

Correspondence: Anda Kfir, Department of Endodontology, School of Dental Medicine, Tel Aviv University, Ramat Aviv, Tel Aviv 62646, Israel (Fax: 972 3 6409250; e-mail: dr.andakfir@gmail.com).

- 3D printed plastic models may be a valuable aid in the process of assessing and planning effective treatment modalities and practicing them *ex vivo* before actually performing the clinical procedure.
- Unconventional technological approaches may be required for detailed treatment planning of complex cases of dens invaginatus.

Keywords: cone beam computed tomography, dens invaginatus, 3 dimensional model, stereolithography.

Received 14 February 2012; accepted 24 August 2012

Introduction

Dens invaginatus is a dental developmental abnormality resulting from the invagination of the enamel organ into the dental papilla prior to the mineralization phase (Shafer *et al.* 1983, Hülsmann 1997, Reddy *et al.* 2008). The cavity that forms may serve as an external route of communication with the pulp or even with the periapical tissues through the foramen caecum. The precise aetiology of dens invaginatus is controversial. A number of theories have been proposed regarding the pathogenesis of dens invaginatus, including uncontrolled growth of a portion of the enamel epithelium (Kronfeld 1934), tooth bud infection during tooth development (Fischer 1936), pressure from the adjacent developing tooth germ (Atkinson 1943), trauma (Gustafson & Sundberg 1950) and genetic components (Grahnen *et al.* 1959, Hosey & Bedy 1996, Dassule *et al.* 2000). Nevertheless, the exact aetiology remains uncertain.

Dens invaginatus is a relatively common condition with a reported incidence ranging from 0.3% to 10% of all teeth (Atkinson 1943, Boyne 1952, Hamasha & Al-Omari 2004). The wide ranges of prevalence quoted in the literature result most probably from variations in the study designs as well as the use of different diagnostic methods and study populations. The permanent maxillary lateral incisors are the most frequently involved teeth (Shafer *et al.* 1983, Hamasha & Al-Omari 2004), with the maxillary central incisors as the second most common area of involvement (Yeh *et al.* 1999). Multiple dens invaginatus involving all four maxillary incisors has been reported (Cronklin 1978). Bäckman & Wahlin (2001) reported a diagnosis of dens invaginatus in combination with other dental malformations.

The clinical appearance of the crown in dens invaginatus varies considerably; the morphology may be normal or it may display unusual forms, such as a peg shape, barrel shape or talon cusps (Ridell *et al.* 2001, Reddy *et al.* 2008). The first clinical sign of an invaginated tooth might be a deep foramen caecum lined by hypomineralized brittle enamel where caries can rapidly develop, enabling microorganisms from the oral cavity to directly penetrate into the pulp, causing pulp necrosis and the development of apical periodontitis (Jung 2004).

The most clinically relevant and widely used classification system for dens invaginatus was proposed by Oehlers (1957): Type I – an enamel-lined minor form, not extending beyond the cemento–enamel junction. Type II – an enamel-lined form that invades the root but remains confined as a blind sac. The invagination may or may not communicate with the dental pulp. Type III – an invagination that penetrates through the root and communicates directly with the periodontal ligament laterally (Type IIIa) or at the apical foramen (Type IIIb). In such cases, there may be no immediate communication with the pulp. In this type, infection within the invagination can cause an inflammatory response in the periodontal or periapical tissues (Alani & Bishop 2008).

On the basis of the diagnosis and treatment plan, different treatment modalities are available, ranging from prophylactic treatment of the deep foramen caecum (Jung 2004), conservative restorative treatment (Hülsmann 1997), nonsurgical root canal treatment (Rotstein *et al.* 1987, Szajkis & Kaufman 1993), endodontic surgery (Soares *et al.* 2007, Vier-Pelisser *et al.* 2012), intentional replantation and extraction (Hata & Toda 1987, Sousa & Bramante 1998, Tsurumachi *et al.* 2002a,b, De Martin *et al.* 2005).

Radiography has an important role in the diagnosis and assessment of the irregular morphology of the root canal system, but conventional planar radiography only provides a two-dimensional representation of the complex anatomy (Patel 2010, Durack & Patel 2011, Vier-Pelisser *et al.* 2012). The limited two-dimensional representation might not yield sufficient information for the clinician to diagnose the true anatomy of the dens invaginatus, thus hindering the effective management of the case.

Cone beam computed tomography (CBCT) provides three-dimensional (3D) undistorted images of the maxillofacial skeleton, including the teeth and their surrounding tissues, and this technique has demonstrated efficacy in a large number of endodontic applications, including but not limited to complex dental anatomy (Patel *et al.* 2009, Al-Rawy *et al.* 2010, Patel 2010, Durack & Patel 2011). Although the effective radiation dose used in CBCT is higher than that of conventional radiographic techniques, it is substantially lower compared to conventional CT (Arai *et al.* 2001, Ngan *et al.* 2003, Ludlow *et al.* 2006, Ludlow *et al.* 2006, Patel & Dawood 2007).

The scanned volume derived from the CBCT software may allow generation of images in three planes that can be continuously scrolled through, thus allowing a three-dimensional understanding of the structure involved. They can also be converted into additional types of files. One of the new types of files that can be derived from the CBCT scans is the stereo litography (STL) file. An STL file is a format used by stereolithography software to generate information needed to produce 3D plastic models using stereolithography machines or printers. Recently, this file format has been used for prototyping and computer-aided manufacturing in other medical fields (Peltola *et al.* 2008).

The aim of this clinical article is to report on the use of a 3D plastic model printed from CBCT digital imaging and communications in medicine (DICOM) data for the diagnosis and conservative treatment of a complex case of dens invaginatus.

Case report

A 15-year-old female was referred to the endodontic department at Goldschleger School of Dental Medicine at Tel Aviv University for treatment of a diffuse periradicular radiolucency around teeth 11 and 12 (Fig. 1). The patient was about to begin orthodontic treatment, and the orthodontic team hoped to maintain the affected tooth, as it was of strategic importance to the patient's maxillary dental arch. Her medical history was unremarkable, and there was no history of dental trauma. The patient reported that the tooth had never been symptomatic.

Clinical examination revealed permanent dentition with teeth 13 and 23, which were in ectopic eruption, and a sinus tract on the labial mucosa near tooth 12 (Fig. 1a), which was traced to tooth 11 (Fig. 1b). Radiographic examination revealed that tooth 11 had a dens invaginatus morphology and had an associated apical radiolucency extending from the mesial aspect of tooth 11 to the distal aspect of tooth 12. The crown of tooth 11 was slightly wider than tooth 21, both mesio-distally and more so bucco-lingually (Fig. 1). A prominent cingulum and a small indication of a foramen caecum were present on the palatal side of the tooth. There were no signs of caries or existing restorations, no discoloration of the tooth and no abnormal mobility. Periodontal probing was within normal limits, and despite the extensive radiolucency, the pulps of teeth 11 and

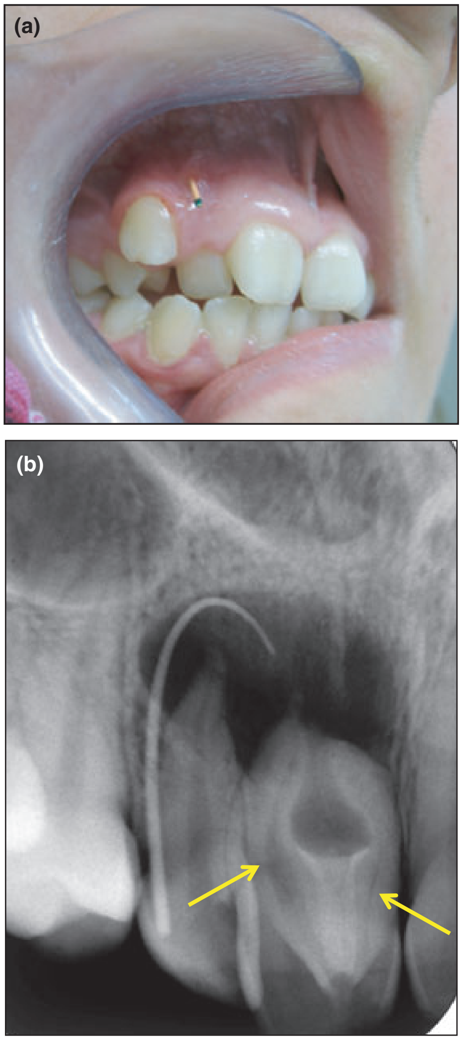

Figure 1 Clinical and radiographic presentation of the case. (a) Sinus tract at the area of tooth 12, traced with a gutta-percha cone. Teeth 11 and 12 were both found to be vital. (b) Periapical radiograph presenting a large radiolucent lesion; a sinus tract traced with a gutta-percha cone. Note the dens invaginatus structure of tooth 11, with a large ballooning space connected to the lesion through a large apical opening. The yellow arrows indicate the pulp space, which was compressed by the invagination.

12 were vital and responded positively to thermal and electric pulp sensitivity testing. The periapical radiograph of tooth 11 presented signs suggesting a class III invagination that appeared to have its own 'apical foramen' (Fig. 1b). Because the morphology of the invagination, the morphology of the pulp canal space and the relationship between the two were not entirely clear from the diagnostic periapical radiograph, it was decided that a limited-volume CBCT scan of the maxilla may be helpful for understanding the internal anatomy of the tooth and determining the most appropriate treatment protocol. The patient and her mother received information on the expected benefits and on the potential risks of the CBCT scan. After obtaining written informed consent, a CBCT (iCAT; Imaging Sciences International, Hatfield, PA, USA) of the maxilla was performed with the following exposure parameters: 120 kV, 3.0 mA and 20 s with field of view of 6 cm. The cross-sectional images revealed a deep invagination surrounded by a thick

layer of calcified tissue. The invagination was completely separated from the root canal, which had a narrow pulp space with one thicker area and a thin crescent-like cross-section. These findings suggested that the pulp space was substantially pushed aside by and currently encircled the invagination (Figs 2 and 3). The invagination presented a substantial ballooning into the walls of the root before tapering to its apical exit. By enhancing the CBCT with a dynamic 3D video, still captures of which are presented in Fig. 3, a clear image of the apical exit of the invagination, its size and its relation to the apical foramen of the main root canal were clearly illustrated.

Tooth 11 was diagnosed as having a vital pulp and a chronic periradicular abscess associated with an infected invagination. The various treatment options were discussed

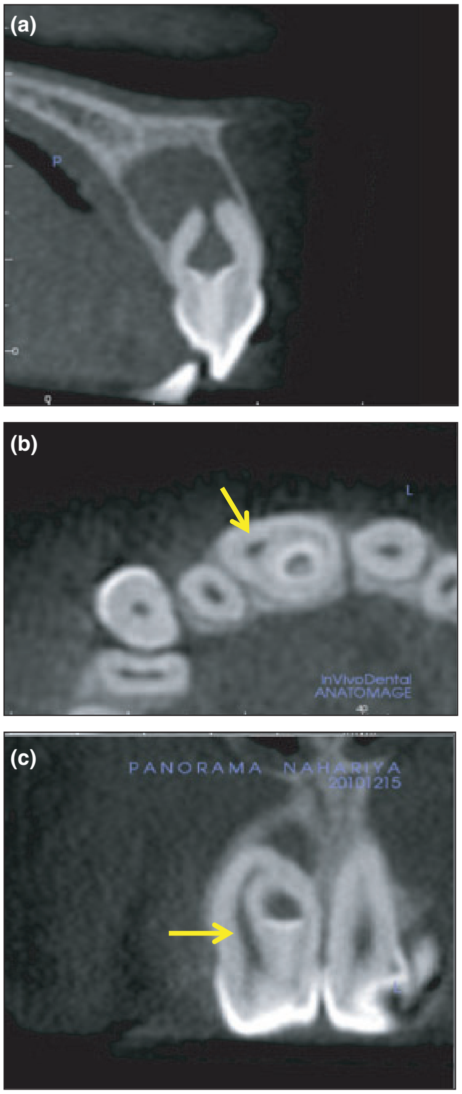

Figure 2 Cone beam computed tomography presentation of the case. (a) Saggital section. Note the large space of the invagination and the extremely compressed pulp space in the buccal side of the root. (b) Axial section. Note the invagination space, which is lined by radiopaque tissue. The yellow arrow indicates the thickest part of the compressed pulp space. Note the asymmetrical shape of the root in the cross-section. (c) Coronal section. The yellow arrow indicates the thickest part of the compressed pulp space.

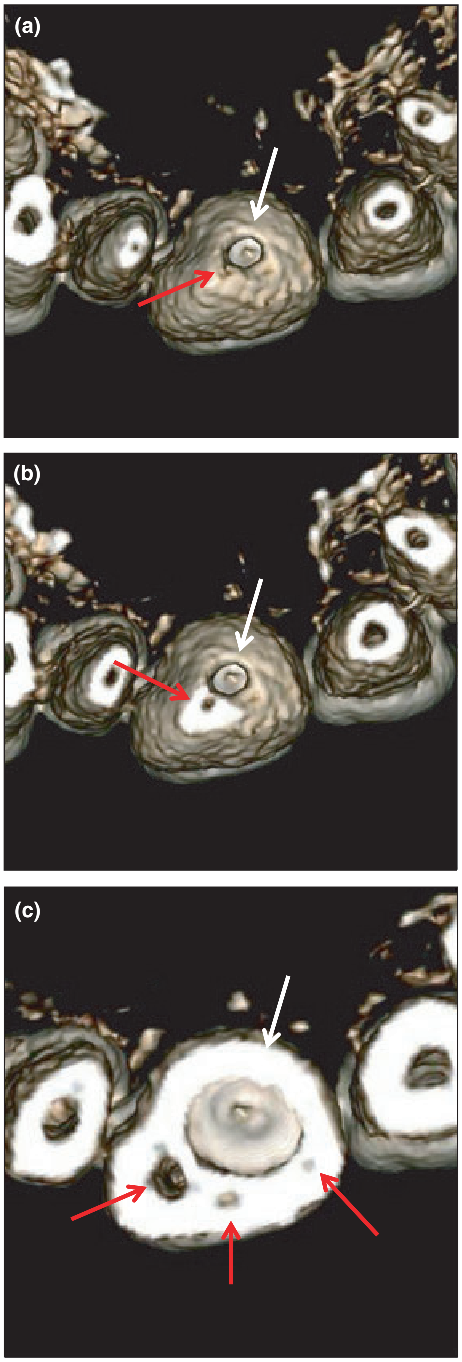

Figure 3 Still captures from a 3D video. (a) Apical view of tooth 11. Note the crater-like apical opening of the invagination (white arrow) and a small depression next to it (red arrow) (b) a more coronal view/section reveals that the small depression seen in 'a' was actually the apical foramen leading to the pulp space. Separation of these two opening explains the vitality of the pulp. (c) A more coronal view/section gives a view of the coronal 'dome' of the invagination and the compressed pulp space. A wide part of the pulp space is seen on the bucco-distal side of the tooth whilst narrower parts are seen on the buccal and mesio-buccal sides. Compare also to Fig. 1b and to Fig. 2b,c.

with the patient and her mother, including conservative treatment as well as a surgical approach and it was decided to treat the infected invagination alone, attempting to leave the vital pulp untreated.

As the morphology of the present dens invaginatus was complex and the pulp was vital, and to avoid unexpected difficulties whilst accessing the invagination and its treatment, a novel therapeutic approach was adopted.

STL files were derived from the CBCT scan data. The scan data were first derived as DICOM3 multiple format which was converted to STL files using Mimics Z software (3DSystems, Rock Hill, SC, USA). The STL files were then subjected to modulation with Geomagic software (Geomagic, Morrisville, NC, USA) and used with a stereolithography 3D printer (Eden 260 V™, Objet Eden 260 V, Objet Inc. Billerica, MA, USA) to generate precise 3D VeroClear™ transparent and FullCure™ opaque plastic 3D models of tooth 11 that included the detailed internal anatomy. The 3D models (prototypes) were printed using a photopolymerized acrylic resin (either VeroClear 810 ™ or FullCure 720 ™ Polyjet resin) that was injected and cured one layer at a time to produce each model at a resolution of $4 \times 42 \times 16$ μ (Erez Rapid Prototyping, Holon Institute of Technology, Holon, Israel). The transparent 3D models (Fig. 4a) were used to study the anatomy of the tooth and enabled the optimal therapeutic approach to be chosen for this complex invagination case. Furthermore, the opaque model (Fig. 4b) was used to practice the techniques required by the different treatment alternatives until sufficient skill was

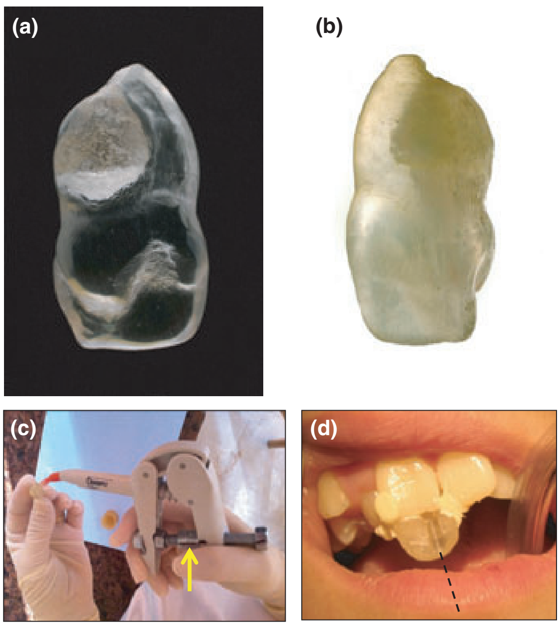

Figure 4 Planning and training for treatment. (a) Lingual view of the transparent VeroClear plastic model. The granular-looking area is the nonsmooth inner surface of the large invagination space. (b) Buccal view of the opaque FullCure model. (c) A modified Compules Syringe (Dentsply Maillefer). The elongation tip of the compule was inserted to a given depth through the access channel of the FullCure model (the tube is not visible in the picture). Note the screw (yellow arrow) that calibrates and limits the amount of mineral trioxide aggregate (MTA) that is delivered into the invagination cavity (Fig. 5a). (d) Drilling guide in position. The acrylic drilling guide was prepared on the transparent VeroClear plastic model to indicate the optimal penetration point and drilling direction that will allow to access the invagination space without passing through or touching the pulp space. The guide was then transferred to tooth 11 and secured in position using some glass–ionomer cement. Drilling was done along the path dictated by the drilling guide (dotted line).

achieved with the filling technique before clinically implementing the procedures (Figs 4c and 5a,b).

Endodontic treatment was carried out over three visits under rubber dam isolation and local anaesthesia with the aid of an operating microscope. The transparent model described earlier revealed that the point of penetration and the direction of drilling to create the access channel would be critical if the pulp was to be preserved. Therefore, an external acrylic drilling-guide device was prepared, which was attached to the tooth during the preparations of access to the invagination cavity (Fig. 4d), thus enabling complete control over the drilling point, direction and depth. At the first visit, the invagination was identified, accessed using a F06RF bur (Strauss & Co., Naharia, Netanya, Israel) using the above-mentioned drilling guide and negotiated with stainless steel hand files (Dentsply Maillefer, Ballaigues, Switzerland). Based on the CBCT data in conjunction with a periapical radiograph, the working length of the invagination was

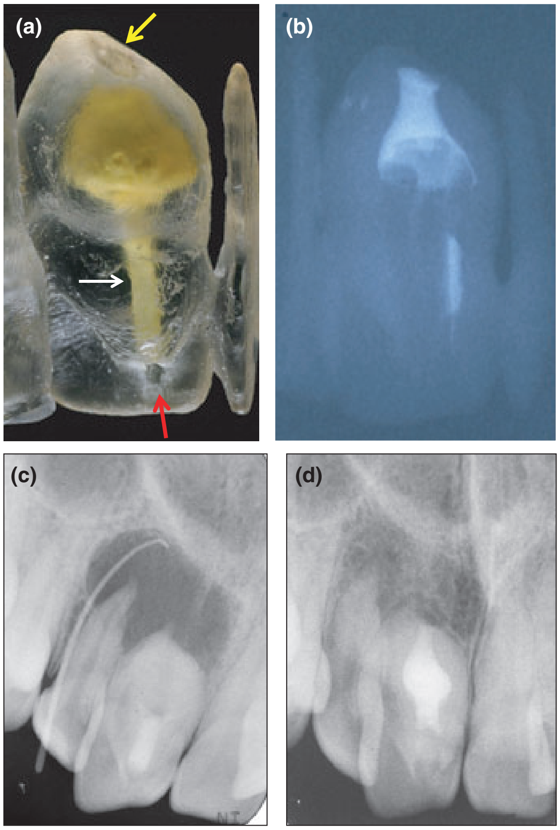

Figure 5 Planning and training for the clinical treatment and its results. (a) The transparent VeroClear plastic model. The area selected for penetration is marked with a red arrow. The direction and depth of the access channel (yellow arrow) were planned on this transparent model and executed with the assistance of an external drilling guide that was also used clinically (Fig. 4d). The access channel and cavity were filled with yellow paste (Ledermix) so that they could be seen in the model. (b) The opaque FullCure plastic model was used for training of the operator in the accurate placement of the MTA. The operator was considered ready to perform the clinical procedure only after radiographic images such as the one shown in B could be reproducibly generated. Note that the FullCure plastic is almost radiolucent. (c) Radiograph taken at the second visit: the sinus tract persisted. The balloon-like radiolucent cavity is not clearly seen due to the radiopacity of the Ledermix that was used as interappointment dressing. (d) Twelve months follow-up. Periapical healing is almost complete. Both teeth 11 and 12 were found to be vital.

established, and its coronal part, up to the ballooned area, was instrumented. The invagination was repeatedly irrigated with copious amounts of 5.25% sodium hypochlorite, which was repeatedly agitated with pre-curved K-files that scrapped the walls, and pre-measured thick gutta-percha master cones that were used to agitate the irrigant. These were done in an attempt to debride and disinfect the ballooned part of the invagination. The invagination was then dried and dressed with Ledermix paste (Haupt Pharma GmbH, Wolfratshausen, Germany) and sealed with a sterile cotton pellet and FUJI IX (GC Corporation, Tokyo, Japan).

Two weeks later, at the second appointment, the patient was asymptomatic. The pulps of teeth 11 and 12 were vital, but the sinus tract was still there (Fig. 5c). The invagination was accessed and again irrigated with large volumes of 5.25% sodium hypochlorite and similar use of bent files, then dressed again with Ledermix paste. At the third appointment, the sinus tract disappeared, whilst the vitality of the pulps in both incisors was maintained.

The planned procedure included filling the invagination with MTA Angelus (Industria de produtos odontologicos Ltd., Londrina, Brazil). To ensure control over the most difficult part of the planned procedure, namely ensuring optimal sealing of the irregular and complex shape of the invagination without pushing the material through the apical opening of the invagination, the placement was first practiced extensively using the 3D plastic model (Fig. 5b). The opaque model was used for this purpose so that the operator could not see the progress of the MTA, mimicking the clinical conditions. The exact amount as well as the proper viscosity of the MTA was tested and calibrated. Due to the unique morphology of the invagination space, MTA guns were too small and ineffective for the treatment of this condition; amalgam carriers could not be inserted to the required point. A special device consisting of a modified Compules Syringe (Dentsply Maillefer) was assembled. An AccuDose® compule (Centrix, Shelton, CT, USA) was adapted with an elongation tip (which is originally designed to be used with Rely X Unichem Aplicap, 3M ESPE, St Paul, MN, USA) that allowed access to the desired depth. The Compules Syringe was adapted with a screw (Fig. 4c) that allowed for calibration and limiting of the amount of injected MTA. This was performed so that it would allow optimal filling of the invagination space without passing the material into the periradicular tissues. Radiographs were used to test the result on the model (Fig. 5b). After the operator had become familiar and fluent with the technique using the model, the MTA filling procedure was performed on the patient. The apical part of the invagination was filled with MTA, including part of the ballooning area. The result was checked radiographically, and the MTA was allowed to set for 15 min. Only then the main part of the invagination was condensed with MTA (Fig. 5d). The access cavity was then restored with a GRADIA composite resin, (GC Corporation). The patient was recalled 6 month later and was asymptomatic. Teeth 11 and 12 responded normally to thermal and electrical sensitivity testing, and a substantial reduction was observed in the size of the periradicular radiolucency. At the next follow-up, at 12 months, the radiograph showed almost complete healing (Fig. 5d) and both teeth responded positively to thermal and electric sensitivity testing.

Discussion

Root canal treatment in teeth with dens invaginatus associated with apical pathosis often involves complicated procedures that require precise diagnosis, appropriate treatment planning and adequate implementation (De Martin *et al.* 2005, Patel 2010). Conventional two-dimensional radiographs have inherent limitations, and their diagnostic yield is further limited by geometric distortion (Gröndahl & Huumonen 2004) and by the lack of information about the third dimension (Patel *et al.* 2009). CBCT has been shown to be useful for assessing the complex anatomy of teeth (Cotton *et al.* 2007, Patel & Dawood 2007, Patel *et al.* 2009, Patel 2010).

Before referring a patient to CBCT, a thorough consideration of risk versus benefit should be performed, especially in a young patient as in the present case. Also the size of FOV (field of view) should be carefully considered. In the present case, 3D imaging was considered essential for treatment planning, but this could have also been achieved with a small FOV. Nevertheless, as the patient had also to go through orthodontic treatment and the orthodontist decided that proper orthodontic assessment of the relation between the roots of the maxillary teeth, in her case, required a larger field of view, it was decided to get a CBCT scan of the entire maxilla, with a 6 cm FOV, to avoid subsequent additional repeated exposure to radiation.

The CBCT scan that was performed in the present case provided a three-dimensional representation of the invaginated tooth and allowed for a true understanding of the nature of the invagination and its relationship to the main canal of the tooth. The CBCT scan was also particularly useful for demonstrating how the invagination compressed the pulp space of the main canal at different levels, resulting in an irregular main canal with a cross-section resembling a thin crescent encircling the invagination, with no communication between the invagination and the pulp space.

The positive response of tooth 11 to vitality testing indicated that the pulp in the main root canal was still viable and presented a normal response to stimuli. Given the complex anatomy of this pulp space, it was considered essential to avoid, as far as possible, perforation of the main root canal or devitalization of the pulp whilst accessing the invagination (Patel 2010). This notion was based on many reports that indicate that pulp spaces with such complex anatomy cannot be expected to be effectively debrided and thus cannot be expected to be adequately obturated (De-Deus *et al.* 2010, 2011, Metzger *et al.* 2010, Solomonov *et al.* 2012).

An alternative treatment plan involving apical surgery was also initially considered and was rejected or at least postponed until the result of the conservative approach could be evaluated. It was estimated that surgical treatment was not the best choice as it would likely lead to devitalization of tooth 12 and would be more traumatic than the conservative approach (Patel 2010, Vier-Pelisser *et al.* 2012).

After adopting the conservative approach, two issues were to be decided: (i) what will be the best path of penetration? (ii) How should the invagination space be cleaned and disinfected?

The printing of a transparent 3D plastic model of this tooth, with its complex invagination, provided an effective means for defining the correct point, direction and depth for the planned access channel, which was created with the assistance of the drilling guide whilst avoiding the viable pulp space (Fig. 4d). The use of this model allowed us to eliminate the trial and error that otherwise would have been required to find access to the invagination. Furthermore, it allowed practice of the treatment modalities before performing the actual procedure on the patient, thus avoiding unexpected complications during implementation. The opaque model (Fig. 4b) was useful in training the operator in placement of the MTA (Fig. 5b). Nevertheless transparent model could also have been used for this purpose by masking it, thus saving 3D printing expenses.

It should be kept in mind that the accuracy of such a procedure, in which CBCT DICOM data are transferred to the STL format may not perfect (Platzer *et al.* 2012). This accuracy may be affected by the type and extent of filtration applied to generate a printable model. In the case at hand, the accuracy was most probably good enough clinically as the drilling guide that was prepared on the printed plastic model had an optimal fit on tooth 11.

Cleaning of the invagination space was performed with copious amounts of sodium hypochlorite, combined with the use of pre-curved hand files that were used to mechanically scrap the internal walls of the invagination space. The use of ultrasonics for this stage was considered and avoided as (i) it may not be effective enough in this kind of balloon-like cavity and (ii) pulp vitality could potentially be risked by local heat generation. Calcium hydroxide was first considered for inter-appointment dressing, but was avoided as it may be extremely difficult to completely remove from such a complex space (Taşdemir *et al.* 2011), thus potentially compromising effective obturation of the invagination space. Ledermix was used as an alternative, as it is easier to remove by irrigation (Rödig *et al.* 2011). The potential staining of an anterior tooth by Ledermix was considered, thus the medicament was carefully removed from the access channel. Nevertheless, as the Ledermix was placed in the invagination channel not in the pulp chamber (which remained vital), penetration of dentinal tubules that may cause such staining was very unlikely (Kim *et al.* 2000, Thomson *et al.* 2012).

Thermoplasticized gutta-percha with sealer is often used when irregular canal spaces are to be filled. In the present case, there was a large apical opening which may have made it difficult to control the apical flow of the softened gutta-percha. MTA was selected as it allowed better apical control (Mohammadi 2011). Furthermore, it was used in two stages, allowing the first layer to set before applying the second one. The MTA Angelus, which has a relatively short setting time, was thus preferred for such procedure (Moore *et al.* 2011).

Cone beam computed tomography involves increased radiation exposure compared to periapical radiography, and therefore, its use should be justified by an analysis and optimization of the risk/benefit ratio for a given patient. In the case reported here, CBCT allowed the operator to make data-based decisions that were essential for treatment planning. Furthermore, the CBCT data could further be enhanced by dynamic evaluation of the full volume of the scan, using the iCat software to allow continuous scrolling in the three planes, thus allowing for in-depth understanding of the intricate anatomical features of this complex case. It allowed also generation of a 3D video, still captures of which are presented in Fig. 3, which also enhanced the understanding of the unique structure of the tooth involved and its surrounding structures. Last but not least, it allowed for stereolithographic printing of 3D plastic models, which provided substantial added value. The endodontic treatment in this case could most probably not have been planned as accurately or performed as safely and successfully without the aid of the CBCT scan.

The process of generation of 3D models from the CBCT data and printing them may sound complicated and costly, thus a little extravagant. Nevertheless, it allowed a conservative treatment plan whilst the alternative treatment plan of apical surgery would have been more traumatic, especially when likely devitalization of tooth 12 is considered. Recruiting the assistance of professionals from other disciplines (3D modelling and printing) proved to be valuable both in clinical and in educational terms. 3D modelling and printing is commonly used in advanced mechanical engineering and the cost in the current case did not exceed 130$ for transfer of the CBCT data into STL files and 100$ for printing the model.

Conclusion

Nonsurgical conservative treatment of a case with complex invagination proved to be successful in promoting the healing of periradicular pathosis, whilst maintaining the viability of the pulp tissue in the main complex canal. Such an option should be considered and attempted as a first choice, irrespective of the size of the periradicular lesion. CBCT is an indispensable tool in the diagnosis and management of invaginated root canals. In complex cases, it may also allow for stereolithographic printing of 3D models to facilitate treatment planning and education.

Acknowledgements

The creative assistance of Eng. Gilad Zelniker and of Mr. Erez Sherman from Erez Rapid Prototyping, Holon Institute of Technology, in printing the 3D plastic models that were used in this study was instrumental to its success and are greatly appreciated.

Disclaimer

Whilst this article has been subjected to Editorial review, the opinions expressed, unless specifically indicated, are those of the author. The views expressed do not necessarily represent best practice, or the views of the IEJ Editorial Board, or of its affiliated Specialist Societies.

References

Alani A, Bishop K (2008) Dens invaginatus. Part 1: classification, prevalence and aetiology. *International Endodontic Journal* **41**, 1123–36.

Al-Rawy B, Hassan B, Vandenberg B, Jacobs R (2010) Accuracy assessment of three-dimensional surface reconstructions of teeth from cone-beam computed tomography scans. *Journal of Oral Rehabilitation* **37**, 352–8.

Arai Y, Honda K, Iwai K, Shinoda K (2001) Practical model '3DX' of limited cone-beam X-ray CT for dental use. *International Congress Series* **1230**, 713–8.

Atkinson SP (1943) The permanent maxillary lateral incisor. *American Journal of Orthodontics* **29**, 685–98.

Bäckman B, Wahlin YB (2001) Variations in number and morphology of permanent teeth in 7-year--old Swedish children. *International Journal of Paediatric Dentistry* **11**, 11–7.

Boyne PJ (1952) Dens in dente: report of three cases. *The Journal of the American Dental Association* **45**, 209–10.

Cotton TP, Geisler TM, Holden DT, Schwartz SA, Schindler WG (2007) Endodontic applications of cone-beam volumetric tomography. *Journal of Endodontics* **9**, 1211–32.

Cronklin WW (1978) Bilateral dens invaginatus in the mandibular incisor region. *Oral Surgery, Oral Medicine, and Oral Pathology* **45**, 905–8.

Dassule HR, Lewis P, Bei M, Maas R, McMahon AP (2000) Sonic hedgehong regulates growth and morphogenesis of the tooth. *Development* **127**, 4775–85.

De Martin AS, de Silveira Bueno CE, Sandhes Cunha R, Aranha de Aranjo R, Fernandes de Magalhaes Silveira C (2005) Endodontic treatment of dens invaginatus with a periradicular lesion: case report. *Australian Endodontic Journal* **31**, 123–5.

De-Deus G, Barino B, Zamolyi RQ *et al.* (2010) Suboptimal debridement quality produced by the single-file F2 ProTaper technique in oval-shaped canals. *Journal of Endodontics* **36**, 1897–900.

De-Deus G, Souza EM, Barino B *et al.* (2011) The self-adjusting file optimizes debridement quality in oval-shaped root canals. *Journal of Endodontics* **37**, 701–5.

Durack C, Patel S (2011) The use of cone beam computed tomography in the management of dens invaginatus affecting a strategic tooth in a patient affected by hypodontia: a case report. *International Endodontic Journal* **44**, 474–83.

Fischer CH (1936) Zur frage des dens in dente. *Deutsche Zahn-, Mundund Kieferheilkunde* **3**, 621–34.

Grahnen H, Lindahl B, Omnel K (1959) Dens invaginatus. I. A clinical, roentgenological and genetical study of permanent upper lateral incisor. *Odontologisk Revy* **10**, 115–37.

Gröndahl H-G, Huumonen S (2004) Radiographic manifestations of periapical inflammatory lesions. *Endodontic Topics* **8**, 55–67.

Gustafson G, Sundberg S (1950) Dens in dente. *British Dental Journal* **88**, 83–8, 111–22, 144–6.

Hamasha AA, Al-Omari QD (2004) Prevalence of dens invaginatus in Jordanian adults. *International Endodontic Journal* **37**, 307–10.

Hata G, Toda T (1987) Treatment of dens invaginatus by endodontic therapy, apicocurettage, and retrofilling. *Journal of Endodontics* **13**, 469–72.

Hosey MT, Bedy R (1996) Multiple dens invaginatus in two brothers. *Endodontics and Dental Traumatology* **12**, 44–7.

Hülsmann M (1997) Dens invaginatus: aetiology, classification, prevalence, diagnosis, and treatment considerations. *International Endodontic Journal* **30**, 79–90.

Jung M (2004) Endodomtic treatment of dens invaginatus type III with three root canals and open apical foramen. *International Endodontic Journal* **37**, 205–13.

Kim ST, Abbott PV, McGinley P (2000) The effects of Ledermix paste on discoloration of mature teeth. *International Endodontic Journal* **33**, 227–32.

Kronfeld R (1934) Dens in dente. *Journal of Dental Research* **14**, 49–66.

Ludlow JB, Davies-Ludlow LE, Brooks SL, Howerton WB (2006) Dosimetry of 3 CBCT devices for oral and maxillofacial radiology: CB Mercuray, NewTom 3 G and i-CAT. *Dentomaxillofacial Radiology* **35**, 219–26.

Metzger Z, Zary R, Cohen R, Teperovich E, Paqué F (2010) The quality of root canal preparation and root canal obturation in canals treated with rotary versus Self Adjusting Files: a three-dimensional micro-computed tomographic study. *Journal of Endodontics* **36**, 1569–73.

Mohammadi Z (2011) Strategies to manage permanent non-vital teeth with open apices: a clinical update. *International Dental Journal* **61**, 25–30.

Moore A, Howley MF, O'Connell AC (2011) Treatment of open apex teeth using two types of white mineral trioxide aggregate after initial dressing with calcium hydroxide in children. *Dental Traumatology* **27**, 166–73.

Ngan DCS, Kharbanda OP, Geenty JP, Darendeliler MA (2003) Comparison of radiation levels from computed tomography and conventional dental radiographs. *Australian Dental Journal* **19**, 67–75.

Oehlers FA (1957) Dens invaginatus. I. Variations of the invagination process and associated anterior crown forms. *Oral Surgery, Oral Medicine and Oral Pathology* **10**, 1204–18.

Patel S (2010) The use of cone beam computed tomography in the conservative management of dens invaginatus: a case report. *International Endodontic Journal* **43**, 707–13.

Patel S, Dawood A (2007) The use of cone beam computed tomography in the management of external cervical resorption lesions. *International Endodontic Journal* **40**, 818–30.

Patel S, Dawood A, Whaites E, Pitt Ford T (2009) New dimensions in endodontic imaging: part 1. Conventional and alternative radiographic systems. *International Endodontic Journal* **42**, 447–62.

Peltola SM, Melchels FP, Grijpma DW, Kellomäki M (2008) A review of rapid prototyping techniques for tissue engineering purposes. *Annals of Medicine* **40**, 268–80.

Platzer S, Bertha G, Heschl A, Wegscheider WA, Lorenzoni M (2012) Three-dimensional accuracy of guided implant placement: indirect assessment of clinical outcomes. *Clinical Implant Dentistry and Related Research*. Article first published online : 15 DEC 2011, DOI: 10.1111/j.1708-8208.2011.00406.x

Reddy YP, Karpagavinayagam K, Subbarao CV (2008) Management of dens invaginatus diagnosed by spiral computed tomography: a case report. *Journal of Endodontics* **34**, 1138–42.

Ridell K, Mejàra I, Matsson L (2001) Dens invaginatus: a retrospective study of prophylactic invagination treatment. *International Journal of Paediatric Dentistry* **11**, 92–7.

Rödig T, Hirschleb M, Zapf A, Hülsmann M (2011) Comparison of ultrasonic irrigation and RinsEndo for the removal of calcium hydroxide and Ledermix paste from root canals. *International Endodontic Journal* **44**, 1155–61.

Rotstein I, Stabholz A, Heling I, Friedman S (1987) Clinical consideration in treatment of dens invaginatus. *Endodontics & Dental Traumatology* **3**, 249–54.

Shafer WG, Hine MK, Levy B (1983) *A Textbook of Pathology*, 4th edn. Philadelphia, PA: WB Saunders Co.

Soares J, Santos S, Silveira F, Nunes E (2007) Calcium hydroxide barrier over the apical root-end of a type III dens invaginatus after endodontic and surgical treatment. *International Endodontic Journal* **40**, 146–55.

Solomonov M, Paque F, Fan B, Eilat Y, Berman LH (2012) The challenge of C-shaped canal systems: a comparative study of the Self-Adjusting File and ProTaper. *Journal of Endodontics* **38**, 209–14.

Sousa SMG, Bramante CM (1998) Dens invaginatus: treatment choices. *Endodontics and dental Traumatology* **14**, 152–8.

Szajkis S, Kaufman AY (1993) Root infolding treatment: a conservative approach in endodontics. *Journal of Endodontics* **19**, 576–8.

Taşdemir T, Celik D, Er K, Yildirim T, Ceyhanli KT, Yeşilyurt C (2011) Efficacy of several techniques for the removal of calcium hydroxide medicament from root canals. *International Endodontic Journal* **44**, 505–9.

Thomson AD, Athanassiadis B, Kahler B, Walsh L (2012) Tooth discoloration: staining effects of various sealers and medicaments. *Australian Endodontic Journal* **38**, 2–9.

Tsurumachi T, Hayashi M, Takeichi O (2002a) Non-Surgical root canal treatment of dens invaginatus type 2 in a maxillary lateral incisor. *International Endodontic Journal* **35**, 68–72.

Tsurumachi T, Hayashi M, Takeichi O (2002b) Non-Surgical root canal treatment of dens invaginatus type 2 in a maxillary lateral incisor. *International Endodontic Journal* **35**, 310–4.

Vier-Pelisser FV, Pelisser A, Recuero LC, Só MVR, Borda MG, Figuerido AP (2012) Use of cone beam computed tomography in the diagnosis planning and follow up of a type III dens invaginatus case. *International Endodontic Journal* **45**, 198–208.

Yeh SC, Lin YT, Lu SY (1999) Dens invaginatus in the maxillary lateral incisor: treatment of 3 cases. *Oral Surgery, Oral Medicine, Oral Pathology, Oral Radiology, and Endodontology* **87**, 628–31.

